Mutational Profile of Advanced Primary and Metastatic Radioactive Iodine-Refractory Thyroid Cancers Reveals Distinct Pathogenetic Roles for *BRAF, PIK3CA*, and *AKT1*

Julio C. Ricarte-Filho,[1] Mabel Ryder,[1,2] Dhananjay A. Chitale,[3] Michael Rivera,[3] Adriana Heguy,[1] Marc Ladanyi,[1,3] Manickam Janakiraman,[1] David Solit,[1,2] Jeffrey A. Knauf,[1,2] R. Michael Tuttle,[2] Ronald A. Ghossein,[3] and James A. Fagin[1,2]

[1]Human Oncology and Pathogenesis Program and Departments of [2]Medicine and [3]Pathology, Memorial Sloan-Kettering Cancer Center, New York, New York

Abstract

Patients with poorly differentiated thyroid cancers (PDTC), anaplastic thyroid cancers (ATC), and radioactive iodine-refractory (RAIR) differentiated thyroid cancers have a high mortality, particularly if positive on [^{18}F]fluorodeoxyglucose (FDG)-positron emission tomography (PET). To obtain comprehensive genetic information on advanced thyroid cancers, we designed an assay panel for mass spectrometry genotyping encompassing the most significant oncogenes in this disease: 111 mutations in *RET, BRAF, NRAS, HRAS, KRAS, PIK3CA, AKT1*, and other related genes were surveyed in 31 cell lines, 52 primary tumors (34 PDTC and 18 ATC), and 55 RAIR, FDG-PET-positive recurrences and metastases (nodal and distant) from 42 patients. *RAS* mutations were more prevalent than *BRAF* (44 versus 12%; $P = 0.002$) in primary PDTC, whereas *BRAF* was more common than *RAS* (39 versus 13%; $P = 0.04$) in PET-positive metastatic PDTC. *BRAF* mutations were highly prevalent in ATC (44%) and in metastatic tumors from RAIR PTC patients (95%). Among patients with multiple metastases, 9 of 10 showed between-sample concordance for *BRAF* or *RAS* mutations. By contrast, 5 of 6 patients were discordant for mutations of *PIK3CA* or *AKT1*. *AKT1*_G49A was found in 9 specimens, exclusively in metastases. This is the first documentation of *AKT1* mutation in thyroid cancer. Thus, RAIR, FDG-PET–positive metastases are enriched for *BRAF* mutations. If *BRAF* is mutated in the primary, it is likely that the metastases will harbor the defect. By contrast, absence of *PIK3CA/AKT1* mutations in one specimen may not reflect the status at other sites because these mutations arise during progression, an important consideration for therapies directed at phosphoinositide 3-kinase effectors. [Cancer Res 2009;69(11):4885–93]

Introduction

Despite the favorable prognosis of well-differentiated thyroid cancer (WDTC), ~5% of them progress to radioactive iodine-refractory (RAIR), [^{18}F]fluorodeoxyglucose (FDG)-positron emission tomography (PET)-positive disease, which commonly leads to death within 5 years. The histology of RAIR, FDG-PET–positive thyroid carcinomas at metastatic and primary sites has been characterized; 50% are poorly differentiated thyroid cancers (PDTC), 23% well-differentiated papillary thyroid cancers (WD-PTC), and 20% tall cell variant PTC (TCV-PTC; ref. 1). Anaplastic carcinomas are invariably RAIR and have a median survival of 0.5 years. Conventional treatment is of marginal benefit for advanced thyroid cancers, emphasizing the importance of developing novel effective therapies.

Progress in our understanding of the genetic alterations underlying the development of thyroid cancer has opened the way for patient-specific therapy by targeting the mutated genes that are causally implicated in this disease. In PTC, nonoverlapping mutations of *RET, NTRK, RAS*, and *BRAF*, genes encoding effectors that activate mitogen-activated protein kinase (MAPK), are found in ~70% of cases (2–4). *RAS* mutations are also found in 50% of follicular thyroid cancers (FTC), which together with *PAX8/PPARγ* rearrangements are seen in 85% of these tumors (5). PDTC and anaplastic thyroid cancers (ATC) can arise from preexisting WDTC, particularly from PTC. Accordingly, mutations of genes considered to be early events in development of WDTC are also found in PDTC and ATC. Indeed, *RET* rearrangements and mutations of *RAS* and *BRAF* are found in PDTC (13%, 46-55%, and 12-17%, respectively), whereas the latter two have been detected in ATC (6-52% and 25-29%; refs. 6–9). Alterations of effectors of the phosphoinositide 3-kinase (PI3K) signaling pathway, *PIK3CA* and *PTEN*, have also been found in thyroid cancer. In contrast to oncogenes encoding MAPK effectors, these genetic alterations are commonly associated with the later stages of thyroid malignant progression, being more frequent in ATC (16% and 14%, respectively) than in WD-PTC (2% and 2%, respectively) or FTC (8% and 7%, respectively; ref. 10). Recently, a transforming mutation (E17K) in the pleckstrin homology domain of the *AKT1* gene has been detected in breast, colon, ovarian, and lung cancers (11–13). Alterations of *PIK3CA, PTEN*, and *AKT1* are mutually exclusive in breast cancer (11, 12). To our knowledge, there are no studies examining the prevalence of *PIK3CA* and *AKT1* mutations in PDTC. A single study investigating for *AKT1* mutations in FTC and ATC yielded negative findings (14).

Compounds that target oncoproteins in the MAPK and PI3K pathways are currently in preclinical and clinical development. It is likely that mapping of genetic alterations in cancer specimens will help determine how patients should be treated. This is particularly important in RAIR cancers, and even more so in those that are also FDG-PET positive, as these are in greatest need of new effective therapies. We designed a thyroid cancer-dedicated platform for matrix-assisted laser desorption/ionization time-of-flight mass spectrometry genotyping (Sequenom) of a comprehensive set of

Note: Supplementary data for this article are available at Cancer Research Online (http://cancerres.aacrjournals.org/).

Requests for reprints: James A. Fagin, Department of Medicine and Human Oncology and Pathogenesis Program, Memorial Sloan-Kettering Cancer Center, 1275 York Avenue, New York, NY 10065. Phone: 646-888-2136; Fax: 646-422-0675; E-mail: faginj@mskcc.org or Ronald A. Ghossein, Department of Pathology, Memorial Sloan-Kettering Cancer Center, 1275 York Avenue, New York, NY 10065. E-mail: ghosseir@mskcc.org

doi:10.1158/0008-5472.CAN-09-0727

oncogenic mutations. This method for high-throughput genotyping is very sensitive for detection of sequence alterations (15, 16). This may be important for detection of mutations in advanced thyroid cancers, which commonly have intermingled stromal tissue, including massive infiltration of tumor-associated macrophages (17). Here, we focused on genotyping "druggable" oncogenes encoding signaling effectors in MAPK and PI3K pathways in advanced thyroid cancers.

Materials and Methods

Histopathologic Analysis

Tumors were classified according to WHO 2004 criteria with the exception of TCV-PTC and PDTC. PDTC were defined by proliferative grading features: ≥5 mitoses/10 high-power fields and/or tumor necrosis regardless of architectural pattern (18). This definition differs from the most recent Turin proposal that requires the presence of a solid/trabecular/insular growth pattern in addition to proliferative grading (19). Tumors were classified as TCV if they contained ≥50% tall cells. The predominant type of tumor cells present in the PDTC was classified as papillary-like, follicular-like, tall cell, or oncocytic.

Thyroid Cancer Tissues and Cell Lines Studied

We analyzed 52 primary tumors (34 PDTC and 18 ATC) and 55 recurrent and nodal and/or distant metastatic samples from 42 patients with RAIR, FDG-PET-positive thyroid carcinomas diagnosed between 1983 and 2007 at Memorial Sloan-Kettering Cancer Center. We previously characterized the histopathology of 70 patients with recurrent/metastatic RAIR, FDG-PET-positive thyroid carcinomas (1). A patient was deemed RAIR if they had an elevated serum thyroglobulin with structural disease in the setting of a negative radioiodine diagnostic whole-body scan. A patient was entered in the study if (*a*) he/she had nonradioactive iodine-avid recurrent/metastatic thyroid carcinoma and (*b*) specimen corresponded to a lesion identified as PET-avid within 2 years of tissue harvesting. Paraffin tissue was available from 42 of 70 patients, which are the focus of the current study. We analyzed 55 samples, including 19 distant metastases at the following sites: bone (5), lung (5), mediastinal lymph node (3), brain (2), skin (2), chest wall (1), and pelvic soft tissue (1); 22 neck lymph node metastases; and 14 recurrences: neck soft-tissue (11) and trachea/esophagus (3). The study was approved by the Memorial Sloan-Kettering Cancer Center Institutional Review Board. We also used a panel of 31 thyroid cancer cell lines, which were genetically fingerprinted by either single nucleotide polymorphism-comparative genomic hybridization or polymorphic short tandem repeat and verified to be unique (20). All cell lines were grown according to the recommendations of the suppliers and maintained at 5% CO_2 at 37°C.

Nucleic Acid Extraction

When necessary, samples were macrodissected to have at least 50% of tumor cells. Genomic DNA was extracted from formalin-fixed, paraffin-embedded (FFPE) tissues using the PUREGene Genomic DNA purification kit (Gentra). DNA from cell lines was extracted using Qiagen DNeasy Blood & Tissue Kit (Qiagen) and RNA was isolated using PrepEase RNA Spin Kit (USB). DNA and RNA from frozen tissues were isolated by AllPrep DNA/RNA Mini Kit (Qiagen). RNA extraction from FFPE samples was done using RecoverAll Total Nucleic Acid Isolation Kit (Ambion; ref. 21). DNA/RNA quality was verified by Nanodrop ND-1000 spectrophotometry followed by PCR with primers specific for the glyceraldehyde-3-phosphate dehydrogenase gene.

Mass Spectrometry Genotyping

Selection of thyroid cancer genetic alterations. We assembled a list of genetic alterations in thyroid cancer by searching the Catalogue of Somatic Mutations in Human Cancer[4] and Pubmed[5] databases. These included somatic, nonsynonymous point mutations and small insertions and deletions in coding regions of selected genes. Genotyping assays, including PCR amplification primers and extension primers, were designed using the Sequenom MassARRAY Assay Design 3.1 Software based on sequences obtained from University of California at Santa Cruz genome browser.[6] Two or more independent genotyping assays were designed for the most relevant mutations. Overall, we designed 107 genotyping assays to interrogate 111 coding substitutions in 16 genes: *BRAF, RET, NRAS, HRAS, KRAS, PIK3CA, AKT1, MET, MAP2K1, IKBKB, PIK3R5, PRKCZ, RHEB, RPS6KA3, RPS6KB1*, and *FRAP1* (Supplementary Table S1). As the mass spectrometry assays for codons 12 and 13 of *HRAS* were not informative, we sequenced all the tumors and cell lines for alterations at these sites.

Genotyping PCR and mass spectrometry. The iPLEX assay is a single-base primer extension assay. First, a PCR amplifying fragments of ~100 bp with primers bracketing the mutation is conducted in a multiplex reaction for several products. Next, extension primers designed immediately adjacent to the mutation site prompt extension by one nucleotide depending on the template sequence. The difference in mass between extended products allows distinction of wild-type and mutant alleles.

Multiplexed PCR was done in 5 μL containing 0.1 unit HotStart Taq polymerase (Kapa Biosystems), 10 ng genomic DNA, 2.5 pmol of each PCR primer, and 2.5 mmol deoxynucleotide triphosphate. Thermocycling was done at 95°C for 15 min followed by 45 cycles of 95°C for 20 s, 56°C for 30 s, and 72°C for 30 s. Unincorporated deoxynucleotide triphosphates were deactivated by incubation with shrimp alkaline phosphatase followed by heat inactivation. Single-base primer extension was carried out using 5.4 pmol of each extension primer, 50 mmol of the appropriate deoxynucleotide triphosphate/dideoxynucleotide triphosphate combination, and 0.5 units Thermosequenase DNA polymerase (iPLEX enzyme). Extension reactions were cycled using a 200-short cycle program that uses two cycling loops as follows: denaturation at 94°C, annealing at 52°C for 5 s, and extension at 80°C for 5 s. This is repeated for a total of five cycles and then looped back to a 94°C denaturing step for 5 s and then a further five cycles of annealing and extension. The five annealing and extension steps with the single denaturing step are repeated 40 times, equating to a total of 200 cycles. A final extension is done at 72°C for 3 min and the sample is cooled to 4°C. After the addition of a cation exchange resin to remove residual salt from the reactions, 7 nL of the purified primer extension reaction were loaded onto a matrix pad (3-hydroxypicoloinic acid) of a SpectroCHIP (Sequenom). SpectroCHIPs were analyzed using a Bruker Biflex III matrix-assisted laser desorption/ionization time-of-flight mass spectrometer (SpectroREADER; Sequenom). All results were manually inspected using the Typer 4.0 software.

To ensure that the samples from patients with multiple tumors were properly categorized, we fingerprinted their genomic DNA using a Sequenom panel that interrogates 42 single nucleotide polymorphisms. All fingerprinting mismatches were removed from the analysis.

PCR products of genomic DNA were sequenced using ABI BigDye Terminator chemistry on an ABI 3730 capillary sequencer (Applied Biosystems).

Vector Ligation and Transformation

DNA samples were amplified by PCR using High-Fidelity Taq DNA Polymerase (Invitrogen) and specific primers bracketing the mutation to be analyzed. The purified PCR products were ligated into the pJET1.2/blunt cloning vector using CloneJET PCR Cloning Kit (Fermentas) and the ligation products used to transform DH5α competent bacterial cells (Invitrogen). Positive colonies were screened by colony PCR using High-Fidelity Taq DNA Polymerase (Invitrogen) and analyzed by 2% agarose gel electrophoresis. PCR products of the expected size were sequenced using pJET1.2 sequencing primers.

Screening for *RET/PTC* and *PAX8/PPARγ* Rearrangements

We used tumor cDNA as template for quantitative PCR to analyze for unbalanced expression of exons 10 to 11 relative to 12 to 13 of *RET*, which

[4] http:/www.sanger.ac.uk/genetics/CGP/cosmic/
[5] http://www.ncbi.nlm.nih.gov/sites/entrez/
[6] http://genome.ucsc.edu

flank the rearrangement site in the intron 11. Samples with 12 to 13 > 10 to 11 expression were screened for specific *RET* recombination events using primers bracketing the respective fusion points of *RET/PTC1, RET/PTC2*, and *RET/PTC3* (22). Positive controls were cDNAs from TPC1 cells (that express RET/PTC1), PCCL3 cells expressing RET/PTC2, and a PTC sample expressing RET/PTC3. We screened for the *PAX8/PPARγ* fusion by RT-PCR using primers for all possible transcripts of *PAX8/PPARγ* (23). cDNA from FTC samples harboring the rearrangement were used as positive controls. *GAPDH* was used as internal control. PCR products were resolved by 2% agarose gel electrophoresis and selected cases were sequenced. *RET* rearrangements were analyzed for all cell lines and in tumors that were wild-type for *BRAF* or *RAS*. *PAX8/PPARγ* was analyzed in all cell lines and primary tumors and in metastatic lesions that were wild-type for *BRAF* and *RAS*.

Statistical Methods

Statistical analyses were done using SPSS 14.0 for Windows. Noncontinuous variables were analyzed using Fischer's exact two-sided test and continuous variables were analyzed using unpaired two-sided *t* tests. Survival analyses were done using Kaplan-Meier log-rank tests. Significance was defined as $P < 0.05$.

Results

Overall detection of thyroid cancer genetic alterations in cell lines and human tissues. We used mass spectrometry to screen for 111 known mutations in 16 cancer genes. In addition, *RET/PTC* and *PAX8/PPARγ* fusion oncogenes were evaluated by quantitative PCR using cDNA as template. We analyzed 31 human thyroid cancer cell lines, 52 primary thyroid cancers (34 PDTC and 18 ATC), and 55 recurrent/metastatic samples from 42 patients with RAIR, FDG-PET-positive thyroid carcinomas. Altogether, we found 122 genetic alterations: these corresponded to 22 of 31 (71%) thyroid cancer cell lines, 26 of 34 (76%) PDTC, 13 of 18 (72%) ATC, and 44 of 55 (80%) recurrences/metastases, including *RET* rearrangements and point mutations in the coding regions of *RET, HRAS, KRAS, NRAS, BRAF, PIK3CA, AKT1*, and *MET*. Many of the mutations found by mass spectrometry (all 9 *PIK3CA*, 9 *AKT1*, and a fraction of the *RAS*- and *BRAF*-positive tumors and cell lines) were also analyzed by Sanger sequencing to validate the assays. Sequencing and mass spectrometry were 100% concordant for *BRAF* and *RAS* mutations. *PIK3CA* and *AKT1* mutations were missed by Sanger sequencing in 11% and 60% of the samples, respectively, indicating that matrix-assisted laser desorption/ionization time-of-flight genotyping was more sensitive in finding mutations. We subcloned PCR products from *AKT1* and *PIK3CA*-mutated samples missed by the Sanger approach and sequenced ~20 to 30 clones of each and found that this technique detected as few as 8% (2 of 24 clones) of mutated cells in a specimen (Fig. 1). Many of the alterations found in the cell lines have been previously reported and were useful as positive controls for optimization of our genotyping platform (Supplementary Table S2). Cell line oncogene mutations not previously reported included *BRAF*_T1799A in T235, T238, and KTC2; *NRAS*_A182G in Hth7 and TT2609-C02; *HRAS*_C181A in Hth-112; *MET*_C3029T in ML1; and *PIK3CA*_G1624A in T238. Twenty-one of 31 (68%) thyroid cell lines have a genetic alteration in the MAPK pathway,[7] with *BRAF*_T1799A being the most common (11 of 31, 35%). None of the MAPK alterations overlapped in the cell lines. We also found 3 *PIK3CA* mutations in cell lines, which overlapped with *BRAF* mutation in all cases. A *MET*_C3029T mutation was found in the ML1 FTC cell line and in one case of ATC. The functional consequence of this alteration in the juxtamembrane domain of MET is controversial, because it has been reported as a somatic mutation conferring tumorigenic advantage (24) and as a germ-line polymorphism (25). Two mesothelioma cell lines harboring this mutation were more sensitive to the MET inhibitor SU11274 than wild-type cells (26). By contrast, we found that growth of ML1 cells was refractory to growth inhibition by SU11274 (IC_{50} > 10 μmol/L; data not shown).

We also screened for an activating mutation in exon 2 of *MEK1* (G171T), recently reported in 1% of lung cancers and shown to confer sensitivity to MEK inhibitors. None of the cell lines, primary or metastatic tumors, had this mutation (27). We also screened 13 thyroid cancer cell lines and 36 primary or metastatic PDTC for mutations at 11 additional sites in exons 11 and 15 of *BRAF* as well as 26 *KIT* alterations previously found in other cancers. No mutations were found, suggesting that these particular alterations are absent or uncommon in thyroid cancer.

Genotype of primary PDTC and ATC. The genetic alterations found in primary PDTC and ATC are shown in Fig. 2 and Supplementary Table S3. Eight of 18 ATC were derived from PTC (4 TCV and 4 WD), whereas 10 were of unknown origin. PDTC derivation was as follows: 23 of 34 PTC (2 TCV and 21 WD), 7 of 34 FTC, 3 of 34 Hurthle cell carcinomas (HCC), and 1 mixed HCC/PTC (Supplementary Table S3). MAPK changes were present in 25 of 34 (74%) PDTC and 12 of 18 (67%) ATC. We found *H/K/N-RAS* mutations to be much more prevalent (44%) in PDTC than *BRAF* mutations (12%; $P = 0.002$). Moreover, patients with *RAS*-positive PDTC had a median survival of 6.6 years compared with 3.3 years for *BRAF* ($P = 0.08$). Accordingly, *BRAF*-mutated PDTC were associated with extrathyroidal extension ($P = 0.04$), whereas *RAS* mutations were robustly associated with absence of extrathyroidal extension ($P = 0.002$), consistent with an opposing role of these oncogenes on key prognostic variables in PDTC. Although ATC patients have a rapidly fatal outcome irrespective of tumor genotype, *BRAF* mutations were more common in this aggressive histotype (44%) than in PDTC (12%; $P = 0.02$). Six of 34 (17%) PDTC had unbalanced expression of *RET* exons 10 to 11 versus 12 to 13. One of these cases had a *RET/PTC3* rearrangement, whereas the others probably carry *RET* rearrangements other than *RET/PTC1, RET/PTC2*, or *RET/PTC3* (Supplementary Fig. S1). *RET*-positive tumors were not associated with differences in survival compared with other groups, although they were associated with extrathyroidal extension ($P = 0.01$). Five cases of *RET/PTC*-positive PDTC were derived from PTC and one from a HCC. None of the ATC had *RET* rearrangements and none of the PDTC or ATC had *PAX8/PPARγ* fusion oncogenes.

Histology and genotype of recurrent and metastatic RAIR thyroid cancers. There were 55 recurrent/metastatic samples from 42 patients with RAIR disease (Table 1). Their histology was as follows: 32 of 55 (58%) PDTC, 12 of 55 (22%) TCV-PTC, 7 of 55 (13%) WD-PTC, 3 of 55 (5%) HCC, and 1 of 55 (2%) ATC. Overall, 33 of 42 (79%) patients and 44 of 55 (80%) samples had at least one mutation. *BRAF* mutations were the most frequent, being found alone or associated with another mutation in 62% of the samples, followed by *AKT1* (16%), *RAS* (13%), *PIK3CA* (5%), and *RET/PTC* (4%). The mutation frequency in recurrent/metastatic samples according to histologic subtype is shown in Table 1 and Supplementary Table S4. *BRAF* mutations were the most common

[7] Note: for simplicity, *RET, RAS*, and *BRAF* are described as genes encoding MAPK effectors, although RET and RAS also signal through multiple other pathways.

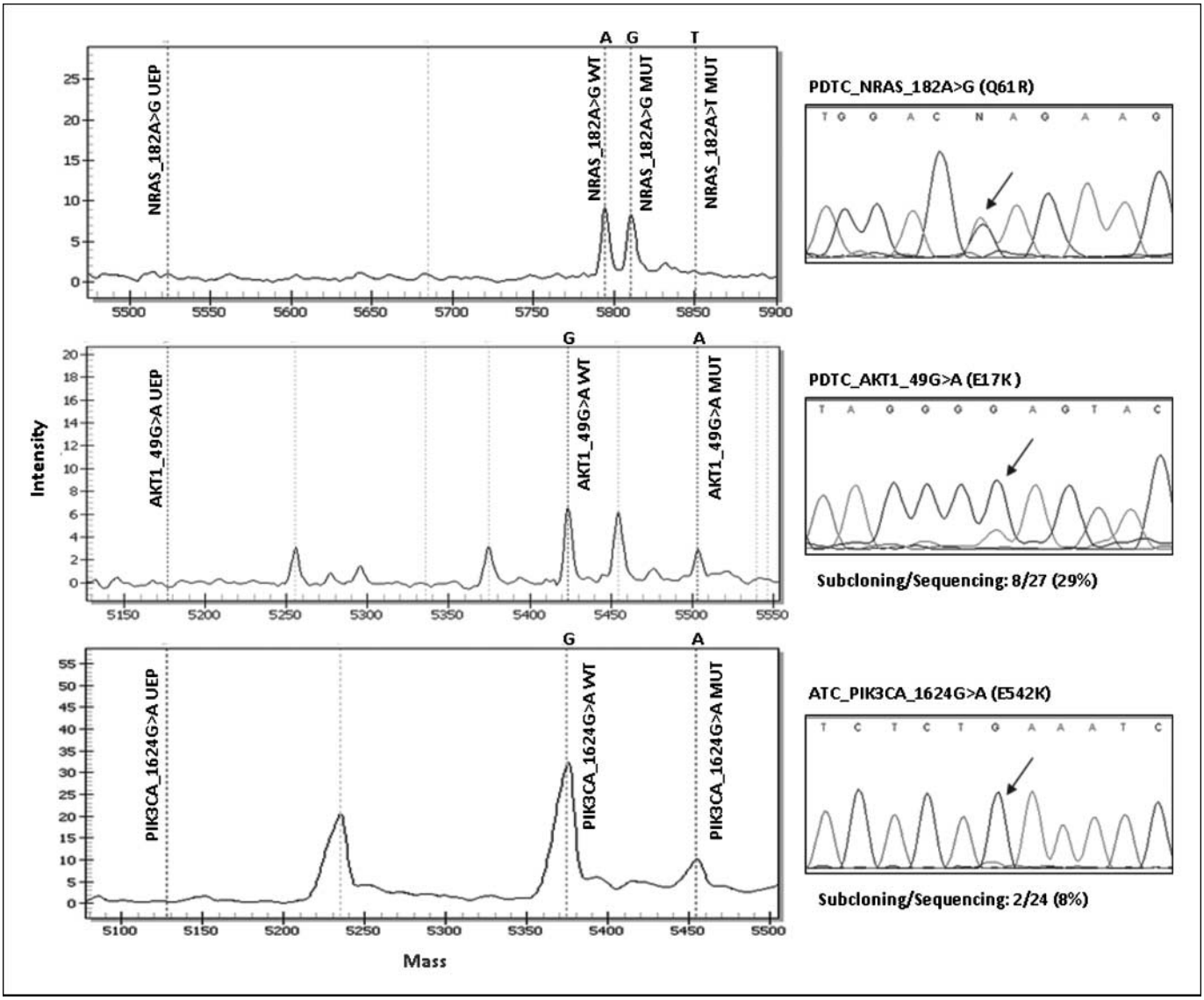

Figure 1. Mass spectrometry (*left*) and Sanger sequencing (*right*) traces of representative samples with *NRAS, AKT1*, and *PIK3CA* mutations. Note that *NRAS* mutant and wild-type peaks are of comparable size, which is also reflected in the sequencing trace. By contrast, the mutant peaks in *AKT1* and *PIK3CA* were small and missed by Sanger sequencing. Subcloning and sequencing detected 8 of 27 (29%) and 2 of 24 (8%) clones to be mutated for *AKT1* and *PIK3CA*, respectively. *WT,* wild-type; *MUT,* mutant; *UEP,* unextended primer.

genetic alteration in PDTC (15 of 32, 47%) and PTC (18 of 19, 95%), the latter including both WD-PTC and TCV-PTC. No differences in genotype were found when comparing recurrences or nodal metastases against distant metastases.

Histology and genotype of FDG-PET–positive recurrent/metastatic lesions. Table 2 shows the histotype and mutational analysis of the 35 recurrent/metastatic RAIR tumors that were also FDG-PET positive. *BRAF* was the most frequently mutated gene, being present in 19 of 35 (54%) samples followed by *RAS* (11%). *BRAF* mutations were detected in all 9 (100%) FDG-PET–positive recurrent/metastatic PTC samples and 9 of 23 (39%) FDG-PET-positive PDTC specimens. All 13 (100%) recurrent/metastatic FDG-PET–positive carcinomas containing significant amount of tall cells (TCV-PTC and some PDTC) harbored *BRAF* mutations, whereas only 6 of 22 (27%) FDG-PET–positive lesions without tall cell features displayed *BRAF* mutations ($P = 0.00002$).

There was a reciprocal relationship in *BRAF* and *RAS* mutation frequency between primary PDTC and FDG-PET–positive PDTC. In primary PDTC, *RAS* > *BRAF* (44% versus 12%; $P = 0.002$), whereas *BRAF* > *RAS* in FGD-PET–positive PDTC (39% versus 13%; $P = 0.04$; Fig. 2). One *RET/PTC2* and one *RET/PTC3* were found among the PET-positive PDTC. These were the only *RET* alterations found in all 55 RAIR recurrent/metastatic samples.

Histopathologic and molecular correlations in patients with multiple tumor specimens. Twelve patients had multiple specimens genotyped (Table 3). For mutations of genes encoding MAPK effectors, 9 of 10 (90%) patients had concordant genotype between the different samples. One patient had the same *RAS* mutation in two metastatic sites. *BRAF* mutations were present in 9 patients. In 8 of these (89%), the *BRAF* mutations were present in all tumor sites tested (Fig. 3). Four of the 12 patients with multiple samples also had specimens of the primary tumor. All

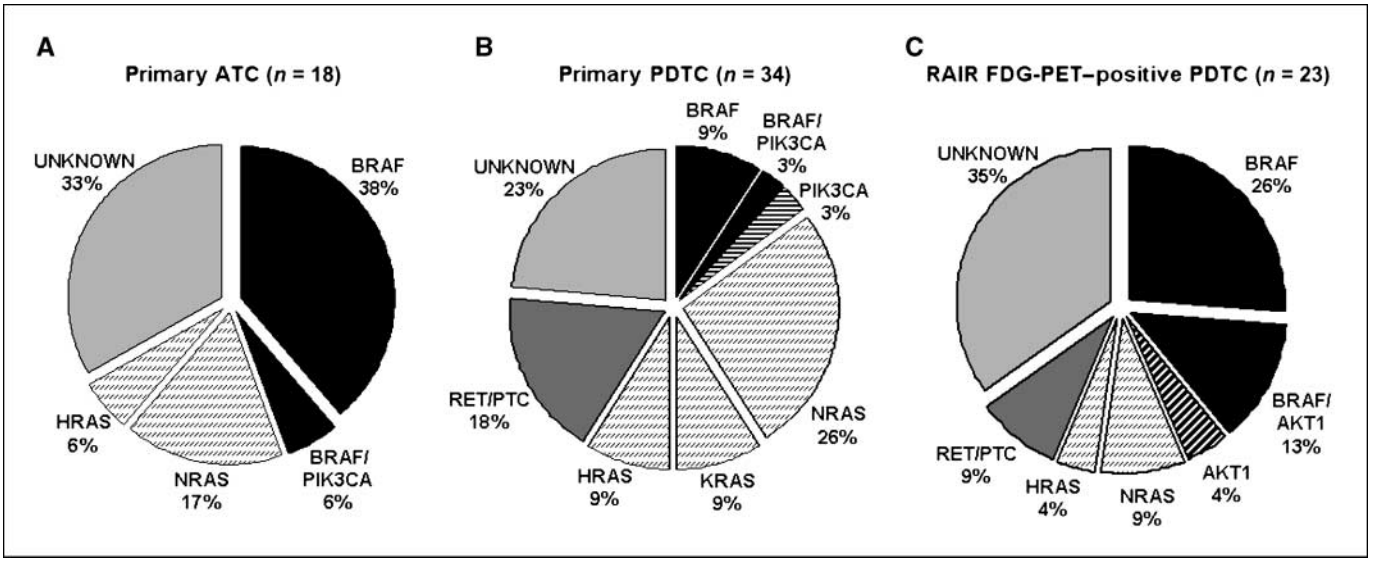

Figure 2. Mutational frequency of *BRAF, RET/PTC, NRAS, HRAS, KRAS, AKT1*, and *PIK3CA* in (*A*) 18 primary ATC, (*B*) 34 primary PDTC, and (*C*) 23 RAIR, FDG-PET–positive PDTC. *RAS* is significantly more prevalent than *BRAF* in primary PDTC ($P = 0.002$) and *BRAF* is more prevalent than *RAS* in RAIR PET-positive PDTC ($P = 0.04$). *RET/PTC* rearrangements were analyzed in cases that were wild-type for *BRAF* and *RAS*.

four had a *BRAF* mutation in primary tumors and at all metastatic sites. As opposed to the concordance of MAPK genetic alterations between samples of individual patients, mutations of genes encoding PI3K pathway effectors (*PIK3CA* and *AKT1*) were discordant in 5 of 6 patients.

***PIK3CA* and *AKT1* oncogenes in advanced thyroid cancer.** Altogether, 9 of 55 (16%) recurrent/metastatic samples from 42 patients with RAIR, FDG-PET–positive thyroid carcinomas had an *AKT1*_G49A mutation (Supplementary Table S4). None of the primary PDTC or ATC or the cell lines harbored this mutation. We found *AKT1* mutations in 6 of 32 (19%) PDTC, 1 of 3 (33%) HCC, and 2 of 12 (17%) TCV-PTC. All but 2 (7 of 9) had a concomitant *BRAF* mutation. This is the first report of *AKT1* mutations in thyroid cancer, and we therefore expanded the analysis to other possible mutation sites and additional samples. The entire exon 1 of *AKT1* was sequenced in all cancer cell lines, PDTC and ATC, as well as 13 follicular adenomas, 12 PTC, and 3 FTC. No further mutations were found. We found 9 samples with *PIK3CA* alterations: 3 thyroid cancer cell lines, 2 primary PDTC, 1 primary ATC, and 3 recurrent/metastatic lesions from patients with RAIR disease: 1 ATC, 1 PDTC, and 1 WD-PTC. *PIK3CA* mutations were found concomitantly with *BRAF* mutations in 8 of 9 cases. Altogether, 15 of 18 (83%) cases with mutations in *PIK3CA* or *AKT1* also had a *BRAF* mutation. We also designed Sequenom assays for other putative oncoproteins in the PI3K pathway discovered as part of the systematic resequencing of other cancer genomes: RHEB_E139K, RPS6KA3_I416V, RPS6KB1_G289E, PIK3R5_R28C, PRKCZ_S514F, IKBKB_A360S, IKBKB_Q611, FRAP1_P2476L, and FRAP1_S2215Y (28, 29). No samples had mutations at any of these sites.

Discussion

The feasibility of using high-throughput matrix-assisted laser desorption/ionization time-of-flight mass spectrometry to genotype patient tumor samples was recently shown in a large survey of multiple tumor types (15). There are few genotyping studies of advanced thyroid cancer, and particularly no comprehensive survey of mutations in primary and metastatic cancers that are RAIR and/or FDG-PET positive, yet these are the tumors most likely to require treatment with kinase inhibitors. These advanced cancers often have features that alter the sensitivity of mutation detection, such as ploidy changes or infiltration with stromal or immune cells (17). We found that sequence alterations present in only 8% of cells were

Table 1. Histotype and genotype of 55 samples from 42 patients with RAIR recurrent/metastatic thyroid carcinomas

Histotype	*n* (%)	*BRAF* (%)	*BRAF-AKT1* (%)	*BRAF-PIK3CA* (%)	*BRAF-NRAS* (%)	*BRAF* total (%)	*NRAS* (%)	HRAS (%)	*RET/PTC* (%)	*AKT1* (%)	Unknown (%)
WD-PTC	7 (13)	4 (57)	—	1 (14)	1 (14)	6 (85)	1 (14)	—	—	—	—
TCV-PTC	12 (22)	10 (83)	2 (17)	—	—	12 (100)	—	—	—	—	—
HCC	3 (5)	—	—	—	—	—	—	—	—	1 (33)	2 (67)
PDTC	32 (58)	9 (28)	5 (16)	1 (3)	—	15 (47)	3 (9)	2 (6)	2 (6)	1 (3)	9 (28)
ATC	1 (2)	—	—	1 (100)	—	1 (100)	—	—	—	—	—
All types	55 (100)	23 (42)	7 (13)	3 (5)	1 (2)	34 (62)	4 (7)	2 (4)	2 (4)	2 (4)	11 (20)

Table 2. Histotype and genotype of 35 RAIR, FDG-PET–positive recurrent/metastatic cases

Histotype	*n* (%)	*BRAF* (%)	*BRAF-AKT1* (%)	*BRAF-PIK3CA* (%)	*BRAF-NRAS* (%)	*BRAF* total (%)	*NRAS* (%)	*HRAS* (%)	*RET/PTC* (%)	*AKT1* (%)	Unknown (%)
WD-PTC	4 (11)	3 (75)	—	—	1 (25)	4 (100)	—	—	—	—	—
TCV-PTC	5 (14)	5 (100)	—	—	—	5 (100)	—	—	—	—	—
HCC	2 (6)	—	—	—	—	—	—	—	—	1 (50)	1 (50)
PDTC	23 (66)	6 (26)	3 (13)	—	—	9 (39)	2 (9)	1 (4)	2 (9)	1 (4)	8 (35)
ATC	1 (3)	—	—	1 (100)	—	1 (100)	—	—	—	—	—
All types	35 (100)	14 (40)	3 (8)	1 (3)	1 (3)	19 (54)	2 (6)	1 (3)	2 (6)	2 (6)	9 (26)

detectable by mass spectrometry but missed by Sanger sequencing. Whereas *BRAF/RAS* mutations were generally detected by both methods, *PIK3CA/AKT1* mutations were often missed by Sanger sequencing possibly because the latter occurs later in tumor progression, when the cancer cells are heavily intermingled with stromal cells. Alternatively, the *PIK3CA* or *AKT1* mutations may be subclonal. This approach allowed us to screen for a large number of genetic alterations simultaneously with enhanced sensitivity, yielding a more comprehensive view of the oncogenic abnormalities in advanced forms of the disease.

The histologic definition of PDTC is controversial, and the few genetic studies of this disease have shown conflicting information. Our analysis shows that PDTC with *BRAF* or *RAS* mutations have distinct biological and clinical behavior. *BRAF* mutations predict for poor outcome in WD-PTC (30), and we now show that this also applies to PDTC. A previous analysis of *RAS* in PDTC showed an association of this oncogene with poor prognosis and aggressive behavior (31). Although this article did not genotype cancers for *BRAF*, this is inconsistent with our observation. This study found a high prevalence of *KRAS* mutations in PDTC, whereas we found mostly mutations in *NRAS*. We are confident about the mutation calls, because we had three assays interrogating *NRAS*_Q61R, and most *KRAS* assays for mutations in codons 12 and 13 were validated in colorectal tumors with positive controls for these alterations. The overall predilection for *NRAS*, as opposed to *KRAS*, mutations in thyroid cancer is also consistent with the Catalogue of Somatic Mutations in Human Cancer database. The differential outcomes of patients harboring cancers with *BRAF* and *NRAS* mutations have been also seen in melanomas (32). Although *RAS* mutations in PDTC indicate a better prognosis, these patients still have a median survival of 6.6 years (1). Currently, there are no effective therapies for tumors harboring

Table 3. Histotype and genotype of 12 patients with multiple tumor specimens

Patient no.	Age, sex	Primary	Rec/met #1	Rec/met #2	Rec/met #3	*BRAF/RAS*	*PIK3CA/AKT1*
1	65, F	PDTC *BRAF*1799T>A	PDTC *BRAF*1799T>A	PDTC *BRAF*1799T>A	NA	Concordant	NA
2	78, F	PDTC *BRAF*1799T>A	PDTC *BRAF*1799T>A	PDTC *BRAF*1799T>A	NA	Concordant	NA
3	49, M	TCV-PTC *BRAF*1799T>A	TCV-PTC *BRAF*1799T>A	TCV-PTC *BRAF*1799T>A	NA	Concordant	NA
4	85, F	TCV-PTC *BRAF*1799T>A	PDTC *BRAF*1799T>A	TCV-PTC *BRAF*1799T>A	NA	Concordant	NA
5	61, M	NA	HCC *AKT1*49G>A	HCC no mutations	NA	NA	Discordant
6	81, F	NA	PDTC *BRAF*1799T>A *AKT1*49G>A	PDTC *BRAF*1799T>A *AKT1*49G>A	NA	Concordant	Concordant
7	67, F	NA	PDTC *NRAS*182A>G	PDTC *NRAS*182A>G	NA	Concordant	NA
8	65, F	NA	PDTC no mutations	PDTC no mutations	NA	NA	NA
9	58, M	NA	PDTC *BRAF*1799T>A *PIK3CA*1624G>A	TCV-PTC *BRAF*1799T>A	NA	Concordant	Discordant
10	49, F	NA	TCV-PTC *BRAF*1799T>A	TCV-PTC *BRAF*1799T>A *AKT1*49G>A	NA	Concordant	Discordant
11	25, M	NA	WD PTC *BRAF*1799T>A *PIK3CA*1624G>A	TCV-PTC *BRAF*1799T>A	NA	Concordant	Discordant
12	25, F	NA	PDTC *HRAS*37G>T	PDTC *RET/PTC2*	PDTC *BRAF*1799T>A *AKT1*49G>A	Discordant	Discordant

Abbreviation: NA, not applicable.

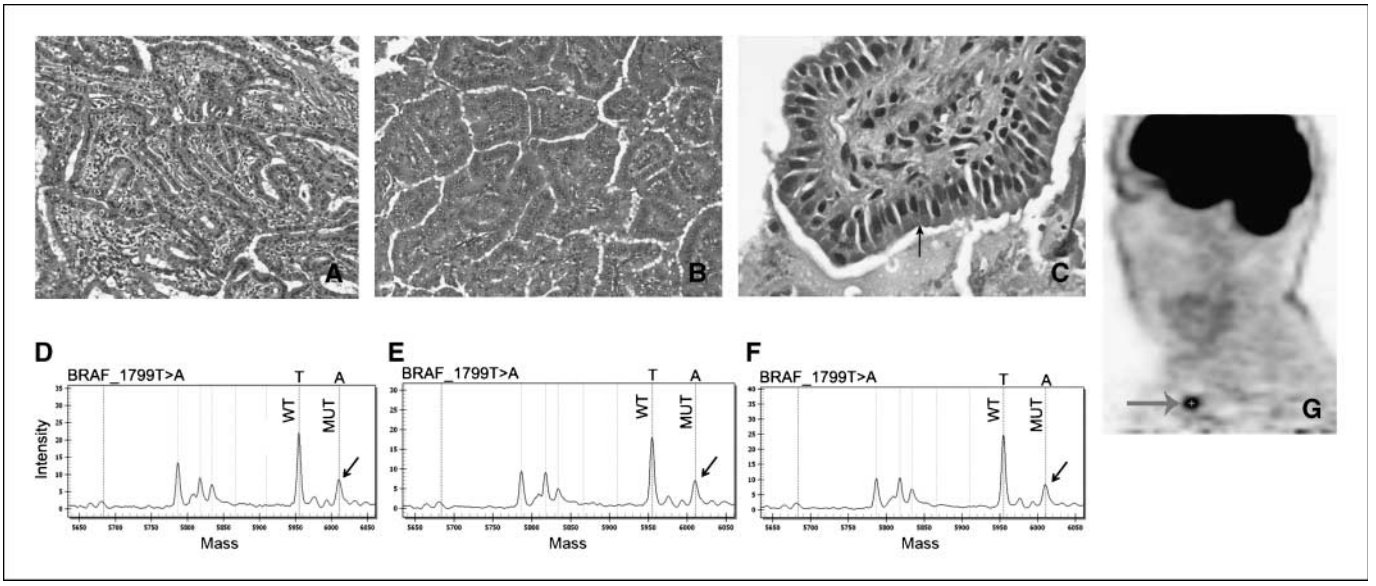

Figure 3. Genotype of multiple tumor sites in a patient with RAIR, FDG-PET–positive thyroid carcinoma. *A,* histology of primary tumor showing TCV-PTC. *B,* histology of metastatic TCV-PTC to lung 15 months after diagnosis. *C,* histology of metastatic TCV-PTC to right supraclavicular lymph node that developed 10 years after removal of primary tumor. This high-power view shows the tumor cells (*arrow*) to be tall (their height at least twice their width) with strong eosinophilic cytoplasm. *D* to *F,* mass spectrometry traces for *BRAF* mutation from primary tumor (*A*), first recurrence (*B*), and second recurrence (*C*), respectively. Note the mutant *BRAF*_T1799A peak (*arrow*). *G,* FDG-PET scan from the second recurrence showing PET-positive lesion (*arrow*) in the right supraclavicular area corresponding to specimen C.

oncogenic *RAS* mutants. A combination of MEK and PI3K/AKT/mammalian target of rapamycin pathway inhibitors is more effective than the respective monotherapy in mouse models of RAS-driven cancers (33–35), raising expectations that this may also be the case in humans.

BRAF mutations were present in 62% of RAIR recurrent/metastatic thyroid carcinomas and in 54% of these tumors that were also FDG-PET positive. The difference in *BRAF* positivity between RAIR tumors and thyroid carcinomas in general is even more marked when comparing these two groups by histotype. Indeed, 100% of FDG-PET–positive RAIR PTC were *BRAF* positive compared with 45% of PTC in general. This is consistent with a previous study of 13 RAIR PTC cases, in which 10 of 13 (77%) PTC harbored *BRAF* mutations (36). The evidence for causality is supported by the fact that conditional activation of $BRAF^{V600E}$ down-regulates expression of the sodium iodide symporter (NIS) in thyroid cells *in vitro* (37). Moreover, human thyroid cancers with *BRAF* mutations show greater reduction of *NIS* mRNA compared with tumors with other mutations or with no identifiable genetic changes (38). This report is the first to show an inordinately high prevalence of *BRAF* mutations in tumors with functional evidence of loss of radioactive iodine avidity. In PDTC, RAIR, FDG-PET–positive tumors harbor *BRAF* mutations in 39% of the samples, whereas *BRAF* is significantly less frequent (12%) in primary PDTC, which more commonly presented with *RAS* mutations (44%). The high frequency of *BRAF* mutation in RAIR, FDG-PET–positive tumors makes *BRAF* an attractive target for therapy to induce cell death and/or to restore radioactive iodine uptake. The putative success of such therapeutic strategies requires that all metastatic or recurrent tumors in the same patient harbor the same genetic defect. *BRAF* mutation is an early event in thyroid cancer pathogenesis (reviewed in ref. 39) and likely to be required for the viability of all subclones of the primary tumor. However, genetic heterogeneity between different primary tumors in multifocal PTC has been reported (40, 41) as well as between primary tumors and regional lymph node metastases (42). By contrast, we found that 8 of 9 patients with *BRAF*-positive cancers had the same *BRAF* mutation in all tumor sites tested. Primary tumors of 4 of 9 of these patients were available, and in all of them, the *BRAF* mutation found in the primary tumor was also present in all metastases. This supports the evidence that *BRAF* is an early event in thyroid carcinogenesis and increases the likelihood that these tumors may be addicted to the oncoprotein.

Most cancers with *RET/PTC* rearrangements are WD-PTC, which are usually not associated with aggressive behavior. Accordingly, we found only two recurrent/metastatic RAIR tumors harboring *RET/PTC* oncogenes. Although rare, this information could be of clinical value as treatment selection becomes more individualized, particularly because multikinase inhibitors with potent activity on RET kinase are entering the clinic (43).

By contrast to *BRAF*, for which primary and metastatic lesions were highly concordant, mutations in *PIK3CA* or *AKT1* were frequently discordant between metastatic samples of the same individuals, consistent with a late acquisition of these oncogenes during tumor progression. Mutations of *AKT1* and *PIK3CA* were mutually exclusive. This is the first report of *AKT1* mutations in this disease. The *AKT1*_G49A mutation was first detected in breast, colon, ovarian, and lung cancers. It constitutively activates AKT signaling and induces leukemia in mice (13). AKT1 activation is associated with tumor invasion in papillary and follicular subtypes of thyroid cancer (44, 45). Moreover, PI3K/AKT activation has been proposed to play an important role in the development of FTC metastasis in $TR\beta^{PV/PV}$ mice, which have homozygous inactivating mutations of the thyroid hormone receptor β (44).

PIK3CA/AKT1 mutations almost invariably coexisted with *BRAF* mutations in our study, pointing to possible cooperativity of coactivation of MAPK and PI3K in disease progression. The

PIK3CA alterations found are within the known hotspots, which have been shown to induce AKT phosphorylation and possess strong oncogenic potential (46). We did not find concomitant alterations in *RAS* and *PIK3CA.* This association has been reported in a subset of anaplastic cancers (9) but, based on the current analysis, is likely to be comparatively infrequent.

Thus, the genotype of primary thyroid cancers for *BRAF* is likely to give an accurate account of the status of this oncogene at metastatic sites. This may not be the case for *PIK3CA* or *AKT1*. This introduces significant caveats to the use of primary cancer specimens for genetic analysis, particularly if patients will be segregated for specific therapies based on this information. This is worth noting in light of the fact that there are many experimental compounds targeting effectors in the PI3K/AKT/mammalian target of rapamycin pathway at various stages of clinical development.

In summary, we show that PDTC with *BRAF* and *RAS* have distinct biological and clinical behaviors. *BRAF* mutations are highly prevalent in FDG-PET7–positive RAIR metastatic thyroid cancers, thus placing this oncoprotein as a prime therapeutic target in the advanced forms of this disease. Mutations of *PIK3CA* and *AKT1*, the latter not previously described in this disease, are comparatively frequent in advanced thyroid cancers, particularly in metastatic or recurrent lesions. *BRAF* mutations are concordant between primary and metastatic specimens, yet this is not the case for *PIK3CA* or *AKT1*, which has implications for our understanding of the sequence of events in thyroid cancer pathogenesis and on how we may apply this information for patient management.

Disclosure of Potential Conflicts of Interest

No potential conflicts of interest were disclosed.

Acknowledgments

Received 2/24/09; revised 4/1/09; accepted 4/6/09.

Grant support: NIH grant CA50706, Margot Rosenberg Pulitzer Foundation, and a Byrne award from Memorial Sloan-Kettering Cancer Center (J.A. Fagin); and CAPES research grant BEX-0644/07-2 (J.C. Ricarte-Filho). The Memorial Sloan-Kettering Cancer Center Sequenom facility is supported by the Anbinder Fund.

The costs of publication of this article were defrayed in part by the payment of page charges. This article must therefore be hereby marked *advertisement* in accordance with 18 U.S.C. Section 1734 solely to indicate this fact.

References

1. Rivera M, Ghossein RA, Schoder H, Gomez D, Larson SM, Tuttle RM. Histopathologic characterization of radioactive iodine-refractory fluorodeoxyglucose-positron emission tomography-positive thyroid carcinoma. Cancer 2008;113:48–56.
2. Kimura ET, Nikiforova MN, Zhu Z, Knauf JA, Nikiforov YE, Fagin JA. High prevalence of BRAF mutations in thyroid cancer: genetic evidence for constitutive activation of the RET/PTC-RAS-BRAF signaling pathway in papillary thyroid carcinoma. Cancer Res 2003;63:1454–7.
3. Soares P, Trovisco V, Rocha AS, et al. BRAF mutations and RET/PTC rearrangements are alternative events in the etiopathogenesis of PTC. Oncogene 2003;22:4578–80.
4. Frattini M, Ferrario C, Bressan P, et al. Alternative mutations of BRAF, RET and NTRK1 are associated with similar but distinct gene expression patterns in papillary thyroid cancer. Oncogene 2004;23:7436–40.
5. Nikiforova MN, Lynch RA, Biddinger PW, et al. RAS point mutations and PAX8-PPARγ rearrangement in thyroid tumors: evidence for distinct molecular pathways in thyroid follicular carcinoma. J Clin Endocrinol Metabol 2003;88:2318–26.
6. Santoro M, Papotti M, Chiappetta G, et al. RET activation and clinicopathologic features in poorly differentiated thyroid tumors. J Clin Endocrinol Metabol 2002;87:370–9.
7. Hou P, Liu D, Shan Y, et al. Genetic alterations and their relationship in the phosphatidylinositol 3-kinase/Akt pathway in thyroid cancer. Clin Cancer Res 2007;13:1161–70.
8. Santarpia L, El-Naggar AK, Cote GJ, Myers JN, Sherman SI. Phosphatidylinositol 3-kinase/akt and ras/raf-mitogen-activated protein kinase pathway mutations in anaplastic thyroid cancer. J Clin Endocrinol Metabol 2008;93:278–84.
9. Garcia-Rostan G, Costa AM, Pereira-Castro I, et al. Mutation of the PIK3CA gene in anaplastic thyroid cancer. Cancer Res 2005;65:10199–207.
10. Paes JE, Ringel MD. Dysregulation of the phosphatidylinositol 3-kinase pathway in thyroid neoplasia. Endocrinol Metab Clin North Am 2008;37:375–87, viii-ix.
11. Stemke-Hale K, Gonzalez-Angulo AM, Lluch A, et al. An integrative genomic and proteomic analysis of PIK3CA, PTEN, and AKT mutations in breast cancer. Cancer Res 2008;68:6084–91.
12. Bleeker FE, Felicioni L, Buttitta F, et al. AKT1(E17K) in human solid tumours. Oncogene 2008;27:5648–50.
13. Carpten JD, Faber AL, Horn C, et al. A transforming mutation in the pleckstrin homology domain of AKT1 in cancer. Nature 2007;448:439–44.
14. Liu Z, Hou P, Ji M, et al. Highly prevalent genetic alterations in receptor tyrosine kinases and phosphatidylinositol 3-kinase/akt and mitogen-activated protein kinase pathways in anaplastic and follicular thyroid cancers. J Clin Endocrinol Metabol 2008;93:3106–16.
15. Thomas RK, Baker AC, Debiasi RM, et al. High-throughput oncogene mutation profiling in human cancer. Nat Genet 2007;39:347–51.
16. Vivante A, Amariglio N, Koren-Michowitz M, et al. High-throughput, sensitive and quantitative assay for the detection of BCR-ABL kinase domain mutations. Leukemia 2007;21:1318–21.
17. Ryder M, Ghossein RA, Ricarte-Filho JC, Knauf JA, Fagin JA. Increased density of tumor-associated macrophages is associated with decreased survival in advanced thyroid cancer. Endocr Relat Cancer 2008;15:1069–74.
18. Hiltzik D, Carlson DL, Tuttle RM, et al. Poorly differentiated thyroid carcinomas defined on the basis of mitosis and necrosis: a clinicopathologic study of 58 patients. Cancer 2006;106:1286–95.
19. Volante M, Collini P, Nikiforov YE, et al. Poorly differentiated thyroid carcinoma: the Turin proposal for the use of uniform diagnostic criteria and an algorithmic diagnostic approach. Am J Surg Pathol 2007;31:1256–64.
20. Schweppe RE, Klopper JP, Korch C, et al. DNA profiling analysis of 40 human thyroid cancer cell lines reveals cross-contamination resulting in cell line redundancy and misidentification. J Clin Endocrinol Metabol 2008;93:4331–41.
21. Li J, Smyth P, Cahill S, et al. Improved RNA quality and TaqMan Pre-amplification method (PreAmp) to enhance expression analysis from formalin fixed paraffin embedded (FFPE) materials. BMC Biotechnol 2008;8:10.
22. Imkamp F, von Wasielewski R, Musholt TJ, Musholt PB. Rearrangement analysis in archival thyroid tissues: punching microdissection and artificial RET/PTC 1-12 transcripts. J Surg Res 2007;143:350–63.
23. Nikiforova MN, Biddinger PW, Caudill CM, Kroll TG, Nikiforov YE. PAX8-PPARγ rearrangement in thyroid tumors: RT-PCR and immunohistochemical analyses. Am J Surg Pathol 2002;26:1016–23.
24. Ma PC, Kijima T, Maulik G, et al. c-MET mutational analysis in small cell lung cancer: novel juxtamembrane domain mutations regulating cytoskeletal functions. Cancer Res 2003;63:6272–81.
25. Schmidt L, Junker K, Nakaigawa N, et al. Novel mutations of the MET proto-oncogene in papillary renal carcinomas. Oncogene 1999;18:2343–50.
26. Jagadeeswaran R, Ma PC, Seiwert TY, et al. Functional analysis of c-Met/hepatocyte growth factor pathway in malignant pleural mesothelioma. Cancer Res 2006;66:352–61.
27. Marks JL, Gong Y, Chitale D, et al. Novel MEK1 mutation identified by mutational analysis of epidermal growth factor receptor signaling pathway genes in lung adenocarcinoma. Cancer Res 2008;68:5524–8.
28. Greenman C, Stephens P, Smith R, et al. Patterns of somatic mutation in human cancer genomes. Nature 2007;446:153–8.
29. Wood LD, Parsons DW, Jones S, et al. The genomic landscapes of human breast and colorectal cancers. Science 2007;318:1108–13.
30. Xing M. BRAF mutation in papillary thyroid cancer: pathogenic role, molecular bases, and clinical implications. Endocr Rev 2007;28:742–62.
31. Garcia-Rostan G, Zhao H, Camp RL, et al. ras mutations are associated with aggressive tumor phenotypes and poor prognosis in thyroid cancer. J Clin Oncol 2003;21:3226–35.
32. Ugurel S, Thirumaran RK, Bloethner S, et al. B-RAF and N-RAS mutations are preserved during short time *in vitro* propagation and differentially impact prognosis. PLoS ONE 2007;2:e236.
33. Downward J. Targeting RAS and PI3K in lung cancer. Nat Med 2008;14:1315–6.
34. Bedogni B, Welford SM, Kwan AC, Ranger-Moore J, Saboda K, Powell MB. Inhibition of phosphatidylinositol-3-kinase and mitogen-activated protein kinase kinase 1/2 prevents melanoma development and promotes melanoma regression in the transgenic TPRas mouse model. Mol Cancer Ther 2006;5:3071–7.
35. Engelman JA, Chen L, Tan X, et al. Effective use of PI3K and MEK inhibitors to treat mutant Kras G12D and PIK3CA H1047R murine lung cancers. Nat Med 2008;14:1351–6.

36. Mian C, Barollo S, Pennelli G, et al. Molecular characteristics in papillary thyroid cancers (PTCs) with no ^{131}I uptake. Clin Endocrinol 2008;68:108–16.

37. Mitsutake N, Knauf JA, Mitsutake S, Mesa C, Jr., Zhang L, Fagin JA. Conditional BRAFV600E expression induces DNA synthesis, apoptosis, dedifferentiation, and chromosomal instability in thyroid PCCL3 cells. Cancer Res 2005;65:2465–73.

38. Durante C, Puxeddu E, Ferretti E, et al. BRAF mutations in papillary thyroid carcinomas inhibit genes involved in iodine metabolism. J Clin Endocrinol Metabol 2007;92:2840–3.

39. Fagin JA. Challenging dogma in thyroid cancer molecular genetics—role of RET/PTC and BRAF in tumor initiation. J Clin Endocrinol Metabol 2004;89:4264–6.

40. Zhu Z, Ciampi R, Nikiforova MN, Gandhi M, Nikiforov YE. Prevalence of RET/PTC rearrangements in thyroid papillary carcinomas: effects of the detection methods and genetic heterogeneity. J Clin Endocrinol Metabol 2006;91:3603–10.

41. Giannini R, Ugolini C, Lupi C, et al. The heterogeneous distribution of BRAF mutation supports the independent clonal origin of distinct tumor foci in multifocal papillary thyroid carcinoma. J Clin Endocrinol Metabol 2007;92:3511–6.

42. Oler G, Ebina KN, Michaluart P, Jr., Kimura ET, Cerutti J. Investigation of BRAF mutation in a series of papillary thyroid carcinoma and matched-lymph node metastasis reveals a new mutation in metastasis. Clin Endocrinol 2005;62:509–11.

43. Santoro M, Carlomagno F. Drug insight: small-molecule inhibitors of protein kinases in the treatment of thyroid cancer. Nat Clin Pract 2006;2: 42–52.

44. Kim CS, Vasko VV, Kato Y, et al. AKT activation promotes metastasis in a mouse model of follicular thyroid carcinoma. Endocrinology 2005; 146:4456–63.

45. Vasko V, Saji M, Hardy E, et al. Akt activation and localisation correlate with tumour invasion and oncogene expression in thyroid cancer. J Med Genet 2004;41: 161–70.

46. Gymnopoulos M, Elsliger MA, Vogt PK. Rare cancer-specific mutations in PIK3CA show gain of function. Proc Natl Acad Sci U S A 2007;104:5569–74.

Mutational Profile of Advanced Primary and Metastatic Radioactive Iodine-Refractory Thyroid Cancers Reveals Distinct Pathogenetic Roles for *BRAF, PIK3CA*, and *AKT1*

Julio C. Ricarte-Filho, Mabel Ryder, Dhananjay A. Chitale, et al.

Cancer Res 2009;69:4885-4893.